

Hydroboration of C(100) Surface, Fullerene, and the Sidewalls of Single-Wall Carbon Nanotubes with Borane

Lasheng Long, Xin Lu,* Feng Tian, and Qianer Zhang

State Key Laboratory for Physical Chemistry of Solid Surfaces & Center for Theoretical Chemistry,
Department of Chemistry, Xiamen University, Xiamen 361005, China

xinlu@xmu.edu.cn

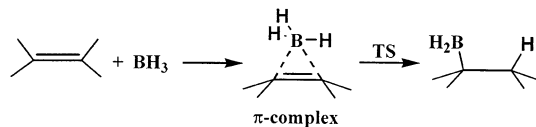
Received March 26, 2003

Hydroboration of three allotropes of carbon, i.e., diamond (100) surface, [60]fullerene, and single-wall carbon nanotubes (SWNTs), with borane (BH_3) has been explored by means of quantum chemical calculations. The calculations predicted that the hydroboration of C_{60} and the C(100)- 2×1 surface occurs readily, whereas the hydroboration of the sidewall of an armchair (5,5) SWNT is thermoneutral with a barrier height of 11.5 kcal/mol. This suggests that sidewall hydroboration, if viable, would be highly reversible on the (5,5) SWNT. The as-hydroborated carbonous materials can be good starting points for further chemical modification and manipulation of these carbonous materials, given the abundant chemistry of organoboranes.

Introduction

The hydroboration of olefins is one of the most important reactions in synthetic organic chemistry, because the so-formed organoboranes are very useful intermediates and are subject to a large number of organic transformations under mild conditions.¹ The prototype reaction is the hydroboration of ethylene (C_2H_4) with borane (BH_3), which produces ethylborane ($\text{C}_2\text{H}_5\text{BH}_2$). The reaction mechanism disclosed by quantum chemical calculations^{2,3} is shown in Scheme 1. This reaction is initiated by electrophilic attack of the electron-deficient boron center of borane to the π -bond of ethylene, forming a π -complex followed by B–H breakage.^{2,3} The absolute rate constant of the reaction of borane with ethylene in the gas phase was first determined by Fehlner⁴ and later by Pasternack et al.⁵ A negative activation energy (-4 kcal/mol) for the overall reaction was suggested by Pasternack et al.⁵ to bring their and Fehlner's data into agreement. Controversy exists in the theoretical predictions of the activation energy of this reaction. While the ab initio SCF calculations overestimated the activation energy with predicted values larger than >4 kcal/mol,³ MP2 calculations with inclusion of correlation energy found no transition state for the reaction.^{3b} Nevertheless, the high reactivity of

SCHEME 1. Hydroboration of Olefins with Borane



borane toward the C–C π -bond in olefins inspires us to consider the feasibility of its possible reactions with fullerene, the diamond (100)- 2×1 surface, and the sidewalls of carbon nanotubes, which are rich in C–C π -bonds.

Indeed, hydroboration of [60]fullerene was found to be facile, occurring at a 6,6 ring fusion C–C bond of C_{60} .⁶ It is well-known that in C_{60} the 6,6 ring fusion C–C bonds are shorter than the 6,5 ring fusion C–C bonds⁷ and can be regarded as a C=C double bond.⁸ This accounts for the high site-selectivity of C_{60} hydroboration.⁶ One purpose of the present work is to explore, by means of quantum chemical calculations, the mechanism of the $\text{BH}_3 + \text{C}_{60}$ reaction and to see to what extent this reaction resembles the prototype $\text{C}_2\text{H}_4 + \text{BH}_3$ reaction.

So far, there has been no report regarding BH_3 reaction with the C(100) surface or with the sidewalls of carbon nanotubes. The reconstructed C(100)- 2×1 surface has a bonding motif in which the adjacent surface carbon atoms are paired up to form symmetric dimers.⁹ The bonding

* Corresponding author. Fax: +86-592-2183047. Phone: +86-592-2181600.

(1) (a) Brown, H. C. *Hydroboration*; W. A. Benjamin: New York, 1962. (b) Brown, H. C. *Acc. Chem. Res.* **1988**, *21*, 287. (c) Pelter, A.; Smith, K.; Brown, H. C. *Borane Reagents*; Batzitzky, A. R., Methcalf, O., Rees, C. W., Eds.; Academic Press: New York, 1988. (d) Matteson, D. S. *Acc. Chem. Res.* **1988**, *21*, 294.

(2) Sundberg, K. R.; Graham, G. D.; Lipscomb, W. N. *J. Am. Chem. Soc.* **1979**, *101*, 2883.

(3) (a) Nagase, S.; Ray, N. K.; Morokuma, K. *J. Am. Chem. Soc.* **1980**, *102*, 4536. (b) Wang, X.; Li, Y.; Wu, Y.-D.; Paddon-Row, M. N.; Rondan, N. G.; Houk, K. N. *J. Org. Chem.* **1990**, *55*, 2601.

(4) Fehlner, T. P. *J. Am. Chem. Soc.* **1971**, *93*, 6366.

(5) Pasternack, L.; Balla, R. J.; Nelson, H. H. *J. Phys. Chem.* **1988**, *92*, 1200.

(6) Henderson, C. C.; Cahill, P. A. *Science* **1993**, *259*, 1885.

(7) (a) David, W. I. F.; Ibberson, R. M.; Mathewman, J. C.; Prassides, K.; Dennis, T. J. S.; Hare, J. P.; Kroto, H. W.; Taylor, R.; Walton, D. R. M. *Nature* **1991**, *353*, 147. (b) Hedberg, K.; Hedberg, L.; Bethune, D. S.; Brown, C. A.; Dorn, H. C.; Johnson, R. D.; de Vries, M. *Science* **1991**, *254*, 410. (c) Yannoni, C. S.; Berthier, P. P.; Bethune, D. S.; Meijer, G.; Salem, J. R. *J. Am. Chem. Soc.* **1991**, *113*, 3190. (d) Disch, R. L.; Schulman, J. M. *Chem. Phys. Lett.* **1986**, *125*, 465.

(8) Fowler, P. W.; Ceulemans, A. *J. Phys. Chem.* **1995**, *99*, 508.

(9) (a) Krüger, P.; Pollmann, J. *Phys. Rev. Lett.* **1995**, *74*, 1155. (b) Furthmüller, J.; Hafner, J.; Kresse, G. *Phys. Rev. B* **1996**, *53*, 7334.

within the surface dimer can be described in terms of a strong σ -bond and a weaker π -bond, analogous to the bonding within the C=C double bond of simple alkenes. Previous experimental and theoretical studies showed that the surface dimers, similar to simple alkenes, are subject to Diels–Alder reactions with conjugated dienes^{10,11} and 1,3-dipolar cycloadditions.¹² Moreover, the π -bonding within the surface dimer is weaker than that in ethylene, due to the nonplanar geometry on the surface dimer, giving rise to a higher reactivity of the surface dimer. Accordingly, we infer that the reaction of BH_3 with the surface dimer would be feasible too, leading to hydroboration of the C(100)-2×1 surface. The second purpose of the present work is to confirm such an inference.

The graphene-like sidewalls of carbon nanotubes display high chemical stability, which impedes the chemical manipulation of carbon nanotubes for further practical uses.¹³ However, the curvature of nanotube sidewalls induces local strain and misalignment of π -orbitals, which would furnish nanotube sidewalls with higher chemical reactivity than that of a flat graphene sheet.¹³ Recent experimental and theoretical studies demonstrated that the sidewalls of single-wall carbon nanotubes (SWNTs) can be covalently functionalized by undergoing [1+2] cycloaddition of nitrenes¹⁴ and 1,3-dipolar cycloadditions of 1,3-dipolar molecules,^{15,16} Diels–Alder cycloaddition of quinodimethane,¹⁷ and base-catalyzed [2+3] cycloaddition of OsO_4 .¹⁸ In these heterogeneous organic reactions, some of the sidewall C–C bonds play the role that a C=C double bond in simple alkenes always does. Considering the high reactivity of BH_3 toward the C=C bond in simple alkenes, we suspect whether analogous reaction can occur on the sidewalls of SWNTs. The third purpose of the present work is to explore the reaction of BH_3 with the sidewalls of SWNTs.

Computational Details

The hybrid density functional theory B3LYP method, i.e., Becke's 3-parameter nonlocal exchange functional¹⁹ with the correlation functional of Lee–Yang–Parr,²⁰ with the standard 6-31G* basis set has been used to study the gas-phase reaction between BH_3 and C_2H_4 (see Figure 1) and the gas–surface reaction between BH_3 and the C(100)-2×1 surface (see Figures

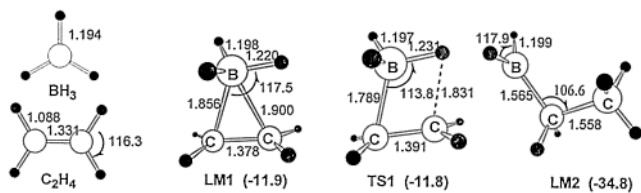


FIGURE 1. B3LYP/6-31G* optimized geometries (units in Å for bond length and deg for angle) of the reactants, intermediate, transition state, and product of the $\text{BH}_3 + \text{C}_2\text{H}_4$ reaction. Energies (kcal/mol) relative to isolated reactants are given in parentheses.

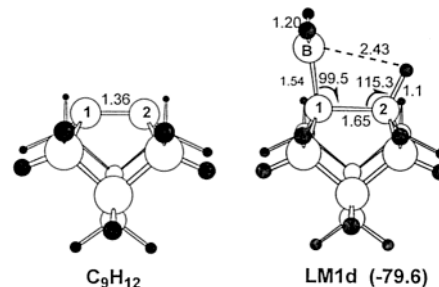


FIGURE 2. B3LYP/6-31G* optimized geometries (units in Å for bond length and deg for angle) of the C_9H_{12} cluster model and the product of the $\text{BH}_3 + \text{C}_9\text{H}_{12}$ reaction. Energy (kcal/mol) relative to isolated reactants is given in parentheses.

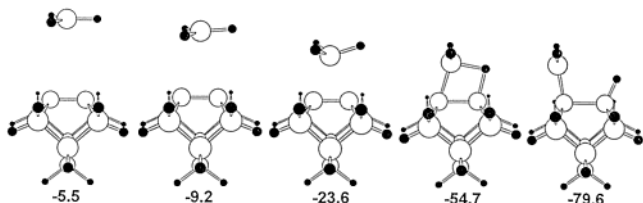


FIGURE 3. A series of geometries on the reaction path for the reaction of BH_3 on the cluster model of the C(100)-2×1 surface. Energies relative to isolated reactants are given in kcal/mol.

2 and 3). A C_9H_{12} cluster model (see Figure 2) has been employed to represent a dimer site on the C(100)-2×1 surface. This cluster model in combination with the B3LYP density functional method was also used in previous theoretical studies of the Diels–Alder cycloaddition¹¹ and 1,3-dipolar cycloadditions¹² on the C(100)-2×1 surface.

A 2-layered ONIOM approach²¹ has been used to study the reactions of BH_3 with C_{60} and SWNT. The semiempirical AM1 method²² and the hybrid density functional B3LYP method^{19,20} together with the standard 6-31G* basis set were employed for the low-level and high-level treatments, respectively. Geometry optimizations were performed within such a 2-layered ONIOM(B3LYP/6-31G*:AM1) approach. Figure 4 shows the architecture of the 2-layered ONIOM model of C_{60} , in which the high-level part is a C_{10} cluster (white circles) in together with eight H atoms as boundary atoms. A similar modeling scheme was used previously in the theoretical prediction of bond-breaking energy in C_{60} by Froese et al.²³

In our study of the reaction of BH_3 with SWNTs, we take the armchair (5,5) SWNT as an example, which was repre-

- (10) (a) Wang G. T.; Bent, S. F.; Russell, J. N., Jr.; Butler, J. E.; D'Evelyn, M. P. *J. Am. Chem. Soc.* **2000**, *122*, 744. (b) Hossain, Z.; Aruga, T.; Takagi, N.; Tsuno, T.; Fujimori, N.; Ando, T.; Nishijima, M. *Jpn. J. Appl. Phys.* **1999**, *38*, L1496.
- (11) (a) Fitzgerald D. R.; Doren D. J. *J. Am. Chem. Soc.* **2000**, *122*, 12334. (b) Okamoto, Y. *J. Phys. Chem. B* **2001**, *105*, 1813.
- (12) (a) Lu, X.; Xu, X.; Wang, N.; Zhang, Q. *J. Phys. Chem. B* **2002**, *106*, 5972. (b) Lu, X.; Xu, X.; Wang, N.; Zhang, Q. *J. Org. Chem.* **2002**, *67*, 515. (c) Lu, X.; Fu, G.; Xu, X.; Wang, N.; Zhang, Q. *Chem. Phys. Lett.* **2001**, *343*, 212.
- (13) Niyogi, S.; Hamon, M. A.; Hu, H.; Zhao, B.; Bhowmik, P.; Sen, R.; Itkis, M. E.; Haddon, R. C. *Acc. Chem. Res.* **2002**, *35*, 1105 and references therein.
- (14) Holzinger M.; Vostrovsky, O.; Hirsch, A.; Hennrich, F.; Kappes, M.; Weiss, R.; Jellen, F. *Angew. Chem., Int. Ed.* **2001**, *40*, 4002.
- (15) (a) Georgakilas, D.; Kordatos, K.; Prato, M.; Guldi, D. M.; Holzinger, M.; Hirsch, A. *J. Am. Chem. Soc.* **2002**, *124*, 760. (b) Georgakilas, V.; Voulgaris, D.; Vazquez, E.; Prato, M.; Guldi, D. M.; Kukovecz, A.; Kuzmany, H. *J. Am. Chem. Soc.* **2002**, *124*, 14318.
- (16) Lu, X.; Zhang, L.; Xu, X.; Wang, N.; Zhang, Q. *J. Phys. Chem. B* **2002**, *106*, 2136.
- (17) Lu, X.; Tian, F.; Wang, N.; Zhang, Q. *Org. Lett.* **2002**, *4*, 4313.
- (18) Lu, X.; Tian, F.; Feng, Y.; Xu, X.; Wang, N.; Zhang, Q. *Nano Lett.* **2002**, *2*, 1325.
- (19) Becke, A. D. *J. Chem. Phys.* **1993**, *98*, 5648.
- (20) Lee, C.; Yang, W.; Parr, R. G. *Phys. Rev. A* **1988**, *37*, 785.

- (21) (a) Maseras, F.; Morokuma, K. *J. Comput. Chem.* **1995**, *16*, 1170. (b) Dapprich, S.; Komáromi, I.; Byun, K. S.; Morokuma, K.; Frisch, M. J. *J. Mol. Struct. (Theochem)* **1999**, *461/462*, 1.
- (22) Dewar, M.; Thiel, W. *J. Am. Chem. Soc.* **1977**, *99*, 4499.
- (23) Froese, R. D. J.; Morokuma, K. *Chem. Phys. Lett.* **1999**, *305*, 419.

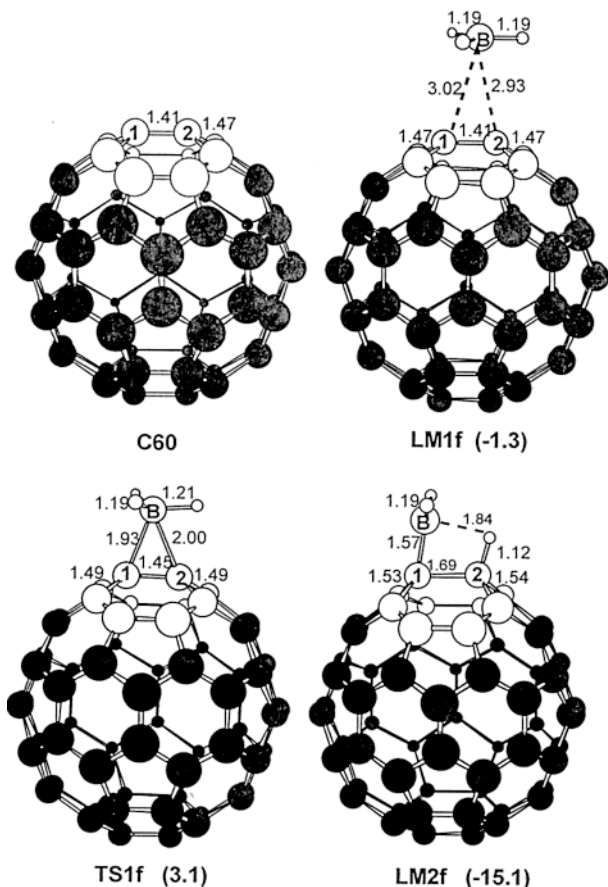


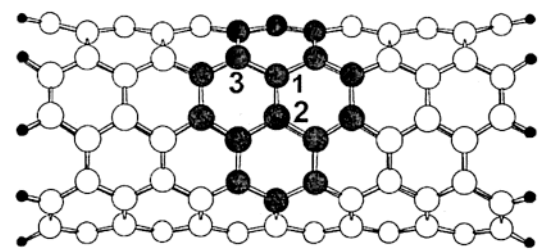
FIGURE 4. ONIOM(B3LYP/6-31G*:AM1) optimized geometries (units in Å for bond length and deg for angle) of C_{60} and the intermediate, transition state, and product of the $BH_3 + C_{60}$ reaction. Energies (kcal/mol) relative to isolated reactants are given in parentheses.

sented by a $C_{130}H_{20}$ model tube (optimal diameter ~ 6.8 Å). Figure 5a shows the $C_{130}H_{20}$ model tube, in which the high-level part is a C_{16} cluster (the shaded atoms in Figure 5a), together with ten H atoms as boundary atoms. Such a modeling scheme was employed in our previous studies of the 1,3-DC of O_3 and Diels–Alder addition of quinodimethane onto the sidewall of (5,5) SWNT.^{16,17} Similar ONIOM modeling was used in many theoretical investigations of carbon nanotube chemistry.^{18,24} On the model tube, only the 1,2 pair site (see Figure 5a) has been considered in the reaction with BH_3 , as our previous study showed this pair site is more ene-like than the 1,3 pair site.¹⁶

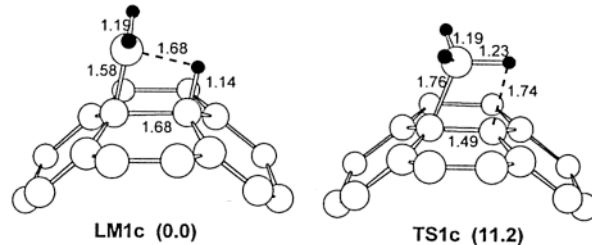
All calculations were performed with use of the Gaussian98 program.²⁵

Results and Discussion

A. $BH_3 + C_2H_4$. The B3LYP/6-31G* optimized geometries of the intermediate (**LM1**) and product (**LM2**) of the gas-phase $BH_3 + C_2H_4$ reaction are depicted in Figure 1, together with the transition state (**TS1**) that connects



(a)



(b)

FIGURE 5. (a) The $C_{130}H_{20}$ model tube to represent the armchair (5,5) SWNT, in which the 16 shaded atoms are used for the high-level treatment in the 2-layered ONIOM(B3LYP/6-31G*:AM1) calculations; (b) ONIOM(B3LYP/6-31G*:AM1) optimized geometries (local views, units in Å for bond length and deg for bond angle) of the product (**LM1c**) and transition state (**TS1c**) for the $BH_3 + (5,5)$ SWNT reaction. Energies (kcal/mol) relative to isolated reactants are given in parentheses.

the intermediate and the product. **LM1** is a π -complex between BH_3 and C_2H_4 with a predicted bonding energy of 11.9 kcal/mol. The product **LM2** is ethylborane, which is predicted to be 34.8 kcal/mol lower in energy than the reactants. The transition state **TS1** is found to be slightly higher in energy than the π -complex, but is 11.8 kcal/mol lower in energy than the reactants. Thus the B3LYP/6-31G* predicted no activation energy for the overall reaction, in agreement with the kinetic experiments reported by Pasternack et al.⁵ In contrast, positive activation energies for the overall reaction were predicted in previous ab initio SCF calculations. Thus, for this gas-phase reaction, our B3LYP/6-31G* calculations and the previous ab initio SCF calculations³ agree in the predicted reaction mechanism, but differ largely in the predicted energetics. The present B3LYP/6-31G* prediction is superior to the previous ab initio SCF predictions regarding the energetics of the $BH_3 + C_2H_4$ reaction.

B. $BH_3 + C_9H_{12}$. The product of the reaction of BH_3 with the dimer of the C_9H_{12} cluster model predicted at the B3LYP/6-31G* level of theory is depicted as **LM1d**

(24) (a) Bauschlicher, C. W. *Chem. Phys. Lett.* **2000**, *322*, 237. (b) Bauschlicher, C. W. *Nano Lett.* **2001**, *1*, 223. (c) Froudakis, G. E. *Nano Lett.* **2001**, *1*, 179. (d) Froudakis, G. E. *Nano Lett.* **2001**, *1*, 531. (e) Froudakis, G. E. *J. Phys.: Condens. Matter* **2002**, *14*, 453. (f) Basiuk, E. V.; Basiuk, V. A.; Banuelos, J.-G.; Saniger-Blesa, J.-M.; Pokrovskiy, V. A.; Gromovoy, T. Yu.; Mischanchuk, A. V.; Mischanchuk, B. G. *J. Phys. Chem. B* **2002**, *106*, 1588. (g) Basiuk, V. A.; Basiuk, E. V.; Saniger-Blesa, J.-M. *Nano Lett.* **2001**, *1*, 657. (h) Basiuk, V. A. *Nano Lett.* **2002**, *2*, 835.

(25) Frisch, M. J.; Trucks, G. W.; Schlegel, H. B.; Scuseria, G. E.; Robb, M. A.; Cheeseman, J. R.; Zakrzewski, V. G.; Montgomery, J. A., Jr.; Stratmann, R. E.; Burant, J. C.; Dapprich, S.; Millam, J. M.; Daniels, A. D.; Kudin, K. N.; Strain, M. C.; Farkas, O.; Tomasi, J.; Barone, V.; Cossi, M.; Cammi, R.; Mennucci, B.; Pomelli, C.; Adamo, C.; Clifford, S.; Ochterski, J.; Petersson, G. A.; Ayala, P. Y.; Cui, Q.; Morokuma, K.; Malick, D. K.; Rabuck, A. D.; Raghavachari, K.; Foresman, J. B.; Cioslowski, J.; Ortiz, J. V.; Stefanov, B. B.; Liu, G.; Liashenko, A.; Piskorz, P.; Komaromi, I.; Comperts, R.; Martin, R. L.; Fox, D. J.; Keith, T.; Al-Laham, M. A.; Peng, C. Y.; Nanayakkara, A.; Gonzalez, C.; Challacombe, M.; Gill, P. M. W.; Johnson, B. G.; Chen, W.; Wong, M. W.; Andres, J. L.; Head-Gordon, M.; Replogle, E. S.; Pople, J. A. *Gaussian 98*; Gaussian, Inc.: Pittsburgh, PA, 1998.

in Figure 2. The reaction is highly exothermic by -79.6 kcal/mol, giving rise to $-\text{BH}_2$ and $-\text{H}$ adspecies. Neither a π -complex nor a transition state has been found for such a gas–surface reaction. Detailed potential energy surface (PES) calculations revealed that such a gas–surface reaction is barrierless, as shown in Figure 3. This clearly shows that the $\text{C}=\text{C}$ dimer on the $\text{C}(100)-2 \times 1$ surface is more reactive than the $\text{C}=\text{C}$ double bond in ethylene. An analogous reaction on the $\text{Si}(100)-2 \times 1$ surface, which has $\text{Si}=\text{Si}$ dimers, was found to be highly exothermic and barrierless by means of density functional cluster model calculations.²⁶

C. $\text{BH}_3 + \text{C}_{60}$. The product of the reaction of BH_3 with the 6,6 ring fusion $\text{C}=\text{C}$ bond predicted at the ONIOM(B3LYP/6-31G*:AM1) level of theory is depicted as **LM2f** in Figure 4. The predicted exothermicity of such a $\text{BH}_3 + \text{C}_{60}$ reaction is -15.1 kcal/mol. To justify the ONIOM approach used, we have calculated the exothermicity of the $\text{BH}_3 + \text{C}_{60}$ reaction purely at the B3LYP/6-31G* level of theory. Full geometry optimizations on C_{60} and **LM2f** were performed at the B3LYP/6-31G* level. The as-predicted exothermicity is -15.0 kcal/mol, showing the ONIOM(B3LYP/6-31G*:AM1) prediction is reliable.

Further ONIOM calculations predicted a weak molecular complex (**LM1f**) of $\text{BH}_3 + \text{C}_{60}$ and a transition state (**TS1f**) that leads to the product, hydroborated C_{60} . In **LM1f**, the closest $\text{C}-\text{B}$ distance is 2.93 \AA . The predicted bonding energy between BH_3 and C_{60} is only 1.3 kcal/mol. The transition state **TS1f** is 3.1 kcal/mol higher in energy than free reactants ($\text{BH}_3 + \text{C}_{60}$). As such, the overall activation energy for the $\text{BH}_3 + \text{C}_{60}$ reaction is 3.1 kcal/mol predicted by the ONIOM(B3LYP/6-31G*:AM1) calculations.

It is interesting to find that the $\text{BH}_3 + \text{C}_{60}$ reaction is neither kinetically nor thermodynamically favorable over the prototype $\text{BH}_3 + \text{C}_2\text{H}_4$ reaction. This can be related to the π -conjugation of C_{60} and high electron deficiency of C_{60} .⁸ C_{60} is known to be highly electron deficient with a high electron affinity of 2.65 eV.²⁷ With an empty p_z atomic orbital at the boron center, BH_3 is also electron deficient. It is not easy for two electron-deficient molecules, i.e., BH_3 and C_{60} , to form a strong dative bond. Thus the bonding in the ($\text{BH}_3 + \text{C}_{60}$) molecular complex **LM1f** is rather weak, while C_2H_4 can form a much stronger $\pi \rightarrow p_z$ dative bond with BH_3 . The electron deficiency of C_{60} makes the $\text{B}-\text{H}$ bond activation more difficult than does C_2H_4 , as the $\text{B}-\text{H}$ bond activation demands electron transfer from C_{60} or C_2H_4 to BH_3 .^{2,3} Hence the $\text{BH}_3 + \text{C}_{60}$ reaction requires an activation energy, while the $\text{BH}_3 + \text{C}_2\text{H}_4$ reaction does not. In the product of the reaction of $\text{BH}_3 + \text{C}_{60}$, the two reacted C atoms adopt sp^3 hybridization, i.e., the reaction leads to a partial destruction of the π -conjugation running around the C_{60} surface. This accounts for the lower exothermicity of the $\text{BH}_3 + \text{C}_{60}$ reaction.

D. $\text{BH}_3 + (5,5) \text{ SWNT}$. The optimized geometries (local views) of the product (**LM1c**) and transition state (**TS1c**) in the reaction of BH_3 with the 1,2 pair site on the sidewall of (5,5) SWNT are depicted in Figure 5b. The reaction gives rise to $-\text{BH}_2$ and $-\text{H}$ adspecies connecting

with two neighboring C atoms on the sidewall. The reacted C atoms thus adopt sp^3 hybridization. As a result, the reacted $\text{C}-\text{C}$ bond in **LM1c** has a bond length of 1.68 \AA , which is the upper limit for a $\text{C}-\text{C}$ single bond. However, the distance between the $-\text{BH}_2$ and $-\text{H}$ adspecies in **LM1c** is only 1.68 \AA , implying substantial interaction between the two adspecies. This structural feature is unique in the hydroborated (5,5) SWNT, as a much longer H to BH_2 distance is found in either the hydroborated C_{60} or the hydroborated $\text{C}(100)$. **TS1c** is a 4-center transition state, similar to those predicted for the $\text{BH}_3 + \text{C}_2\text{H}_4$ reaction and the $\text{BH}_3 + \text{C}_{60}$ reaction. Thus all these reactions adopt similar mechanism for the activation of the $\text{B}-\text{H}$ bond in BH_3 , i.e., upon approach of the BH_3 molecule to the $\text{C}=\text{C}$ bond, electron transfer occurs from the π -bond to the BH_3 molecule, leading to polarization of the $\text{C}-\text{C}$ bond and the $\text{B}-\text{H}$ bond followed by cleavage of the $\text{B}-\text{H}$ bond and formation of $\text{C}-\text{BH}_2$ and $\text{C}-\text{H}$ bonds.

Furthermore, the heterogeneous $\text{BH}_3 + (5,5) \text{ SWNT}$ reaction is predicted to be thermoneutral with an activation energy of 11.2 kcal/mol, suggesting that the sidewall hydroboration of (5,5) SWNT, if viable, would be highly reversible. However, such a thermoneutral reaction seems to be unfavorable in terms of translational entropy. Since the chemical reactivity of the sidewalls of SWNTs depends on the sidewall curvature or/and the diameter of SWNTs, and SWNTs with larger diameters are less reactive,¹³ it is expected that sidewall hydroboration of SWNTs with larger diameters would hardly be viable in practice.

Concluding Remarks

Motivated by the hydroboration chemistry of olefins, we explored theoretically the hydroboration chemistry of three carbon allotropes, i.e., $\text{C}(100)$, [60]fullerene and a single-wall carbon nanotube. Our quantum chemical calculations suggest that the hydroboration chemistry of olefins can be used to chemically functionalize these carbonous materials except SWNTs, leading to $-\text{BH}_2$ and $-\text{H}$ adspecies on the surfaces. Given the as-hydroborated carbonous materials as the starting point for further chemical modification, the abundant chemistry of organoboranes would offer high flexibility in the chemical modification and manipulation of those carbonous materials that are of great importance in industry.

Acknowledgment. This work was sponsored by Fok Ying-Tung Educational Foundation, Nature Science Foundation of China (Nos. 20203013, 20021002, and 20023001), the Ministry of Education of PRC (No. 20010384005), the Ministry of Science and Technology (Nos. G1999022408 and 2002CCA01600), the Natural Science Foundation of Fujian Province (Nos. E0210001 and 2002F010), and Xiamen University.

Supporting Information Available: Cartesian coordinates and total energies in hartrees for the stationary points in the hydroboration reactions concerned. This material is available free of charge via the Internet at <http://pubs.acs.org>.

JO034395R

(26) Konecny, R.; Doren, D. J. *J. Phys. Chem. B* **1997**, *101*, 10983.
(27) Wang, L. S.; Coneicao, J.; Jin, C.; Smalley, R. E. *Chem. Phys. Lett.* **1991**, *182*, 5.